

Generalized fractional grey system models: Memory effects perspective

Wanli Xie^a, Wen-Ze Wu^{b,*}, Chong Liu^{c,**}, Mark Goh^{d,e}

^a*Institute of EduInfo Science and Engineering, Nanjing Normal University, Nanjing 210097, China*

^b*School of Economics and Business Administration, Central China Normal University, Wuhan 430079, China*

^c*School of Science, Northeastern University, Shenyang 110819, China*

^d*NUS Business School, National University of Singapore, 21 Lower Kent Ridge Road, Singapore*

^e*The Logistics Institute-Asia Pacific, National University of Singapore, 21 Lower Kent Ridge Road, Singapore*

Abstract

As an essential characteristics of fractional calculus, the memory effect is served as one of key factors to deal with diverse practical issues, thus has been received extensive attention since it was born. By combining the fractional derivative with memory effects and grey modeling theory, this paper aims to construct an unified framework for the commonly-used fractional grey models already in place. In particular, by taking different kernel and normalization functions, this framework can deduce some other new fractional grey models. To further improve the prediction performance, the four popular intelligent algorithms are employed to determine the emerging coefficients for the UFGM(1,1) model. Two published cases are then utilized to verify the validity of the UFGM(1,1) model and explore the effects of fractional accumulation order and initial value on the prediction accuracy, respectively. Finally, this model is also applied to dealing with two real examples so as to further explain its efficacy and equally show how to use the unified framework in practical applications.

Keywords: Fractional derivative, Memory effect, Grey modeling technique, Unified framework, Intelligent algorithm

1. Introduction

Grey system theory, an effective approach to addressing the issues in uncertain systems, was proposed by Deng [1]. The grey system theory can fully dig out the internal rule of systems with limited data, this enables it has very important application prospects and successfully solved many practical problems. Grey prediction model is the most essential model in the grey system theory, and it has become a research hotspot of scholars in recent years. To be specific, GM(1,1) [2], DGM(1,1) [3] are two kinds of commonly-used grey models, there are many published papers focusing on them [4, 5, 6, 7, 8]. At the same time, the studies related to grey system forecasting models have been still emerged, and the prediction performance of grey forecasting models will be continuously enhanced as well [9, 10]. In order to further improve the accuracy and application range of the grey models already in place, many scholars have proposed several new types of grey prediction models. For example, Lang et al. [11] proposed a

*Corresponding author.

**Corresponding author.

Email addresses: wenzew@mails.cnu.edu.cn (Wen-Ze Wu), liuchong@mails.ima.u.edu.cn (Chong Liu)

new time-lag grey model to forecast photovoltaic power generation in the Asia-Pacific region. Zhou et al. [12] put forward a new discrete grey model for natural gas prediction in Jiangsu Province, China. Wu et al. [13] constructed a new nonlinear grey model for short-term natural gas prediction. Zhou et al. [14] established a novel discrete grey seasonal model and used several practical examples to verify the effectiveness of their model. Wang and Jv [15] combined the grey prediction model and quantile regression so as to design a combination for forecasting time-series sequence. Xiao et al. [16] proposed an optimized nonlinear grey model for biomass energy consumption prediction. Li et al. [17] searched the optimal fractional accumulation order for improved seasonal grey model by virtue of the particle swarm optimization (PSO). Zeng et al. [18] optimized the structure of the grey Verhulst model. Wei and Xie[19] proposed a method family for nonlinear parameter estimation of grey forecasting models, their numerical results show that the proposed method has advantages of high accuracy and robustness. Zeng [20] proposed a novel discrete grey Riccati model and verified its effectiveness in a range of practical application scenarios. Xiao et al. [21] put forward a grey Riccati Bernoulli model and successfully applied it to deal with clean energy consumption. Ye et al. [7] proposed a novel time-delay multivariate grey model And used in China's carbon dioxide analysis.

Admittedly, the above models achieve satisfactory results and address many practical problems, however, the accumulation order in these models are all integer-order, which is prone to impair the prediction performance. In other words, the accumulation order should dynamically alter in accordance with modeling situations. To this end, Wu et al. [10] proposed the fractional gray model in 2013. Subsequently, various extensive forms of fractional models were proposed [22, 23]. At the same time, several other types of fractional accumulation operators have also been proposed, each with its own advantages. Ma et al. [24] proposed a conformable fractional accumulation (denoted as CFA) and built a conformable fractional grey prediction model. Chen et al. [25] incorporated Fractional Hausdorff derivative into the modeling procedure of grey model so as to construct a new method. Liu et al. [26] proposed the damping accumulated generating operator and constructed a new fractional grey model. With the continuous development of fractional grey models, fractional derivatives are applied on the differential equation of grey models [27, 28].

For example, Mao et al. [29] proposed a fractional grey model based on non-singular exponential kernel.

$$\frac{1}{1-r} \int_0^t x'(\tau) \exp\left[-\frac{r(t-\tau)}{1-r}\right] d\tau + ax^{(r)}(t) = b; \quad r > 0, t > 0. \quad (1)$$

where $x^{(r)}(t)$ is the r -order accumulation [10] of the original sequence $x^{(0)}(t)$, and literature [28] proposed a fractional prediction model with conformable derivatives. The research status of fractional grey model can be seen in Table 1. Using different fractional derivatives in the gray model can make full use of different types of derivatives to dig out potential laws among data. Fractional calculus has become a research hotspot of scholars [29]. The famous Riemann-Liouville fractional integral with $r \in \mathbf{R}$ order [30] by

$$I_{t_0, r}^{RL} f(t) = \frac{1}{\Gamma(r)} \int_{t_0}^t (t-\tau)^{r-1} f(\tau) d\tau = \Phi_r * f(t); \quad r > 0, x > t_0, \quad (2)$$

motivated by the Cauchy integral

$$\int_{t_0}^t d\tau_1 \int_{t_0}^{\tau_1} d\tau_2 \cdots \int_{t_0}^{\tau_{n-1}} f(\tau_n) d\tau_n = \frac{1}{\Gamma(n)} \int_{t_0}^t (t-\tau)^{n-1} f(\tau) d\tau. \quad (3)$$

Where $*$ is the convolution operator and Φ_r is the power function $\Phi_r(\tau) = \frac{1}{\Gamma(r)}\tau_+^{r-1}$. Zhao and Luo [30] proposed a generalized fractional operator, which proved that several types of calculus expressions are special cases of this operator.

Table 1: Research findings of the different fractional grey models in recent years.

Author's name(year)	Approach	Abbreviation	FAGO	FD
Wu (2013)[10]	Grey model with the fractional order accumulation	FGN(1,1)	✓	-
Mao (2016)[28]	Fractional grey system model	FGM(q,1)	✓	✓
Yang (2016)[11]	Continuous fractional-order grey model	GM(q,1)/GM(q,N)	-	✓
Yang (2018)[31]	Interval grey modelling based on fractional calculus	Interval GM(1,1)		-
Wu (2018)[32]	The GMC(1,n) model with fractional order accumulation	FGMC(1,n)	✓	-
Wu (2018)[33]	Fractional order accumulation grey model	FAGMO(1,1,k)	✓	-
Ma (2019)[34]	Fractional discrete multivariate grey model	FDGM(1,n)	✓	-
Chen (2019)[35]	Time-delayed polynomial fractional order grey model	TDPFOGM(1,1)	✓	-
Ma (2019)[24]	Conformable fractional grey model	CFGM(1,1)	✓	-
Wang (2019)[36]	Fractional calculus function of grey prediction model	FGM(1,1)	✓	-
Ma (2019)[37]	Fractional time delayed grey model	FTDGM(1,1)	✓	-
Zhu (2019)[38]	Self-adaptive fractional weighted grey model	SFOGM(1,1)	-	-
Yan (2020)[25]	Fractional Hausdorff grey model	FHGM(1,1)	✓	-
Xie (2020)[39]	Continuous grey model with conformable fractional derivative	CCFGM(1,1)	✓	✓
Wu (2020)[13]	conformable fractional non-homogeneous grey model	CFNGM(1,1)	✓	-
Kang(2020)[40]	Fractional derivative multivariable grey model	CFGMC(q,N)	✓	✓
Gao(2020) [41]	fractional grey Riccati model	FGRM(1,1)	✓	-
Mao (2020)[29]	Fractional grey model based on non-singular exponential kernel	EFGM(q,1)	✓	✓
Liu (2021)[26]	The damping accumulated grey model	DAGM	✓	-
Liu (2021)[42]	Optimized fractional grey model-based variable background value	OFAGM(1,1)	✓	-
Zhang (2021)[43]	Fractal derivative fractional grey Riccati model	PDFGRM	✓	✓

Based on the above acknowledge, it is concluded that the fractional grey model has been widely used in diverse fields and a large number of fractional grey models has been constantly emerged. However, in return, there exist a variety of fractional grey models with various constructions of fractional accumulated generating operator, which is not conducive for beginners to understand and grasp the relevant modeling mechanism; at the same time, it is difficult for participants to identify which model can provide satisfactory results in specific scenarios, thus restraining the further methodological developments and

practical applications.

To this end, this paper develops an unified framework for commonly-used fractional grey models by combining general fractional derivative with memory effects and grey modeling theory. The main contributions can be outlined as follows. (i) In accordance with the GC and GRL derivatives, the unified framework for diverse fractional grey model is developed, this framework also derive other new fractional grey models by taking different kernel functions and normalization functions. (ii) The exact solution (often called time response function) and the corresponding estimates of the structural parameters are, in detail, deduced from this proposed framework. (iii) The four popular intelligent algorithms are employed to determine the emerging coefficients r, α . (iv) Two published cases are utilized to verify the effectiveness of the UFGM(1,1) model and especially explore the effects of fractional accumulation order and initial value on the prediction performance. (v) The UFGM(1,1) model is also applied in two real cases to explain how to apply the proposed approach.

The rest of paper is organized as follows: Section 2 briefly introduces general fractional derivatives with memory effects. Section 3 discusses the modeling procedure of the unified framework. Section 4 verifies the validity of the UFGM(1,1) model. Section 5 applies this method in dealing with Henan's and Chongqing's water supply production capacity and Section 6 concludes.

2. General fractional derivatives with memory effects

In this section, we will give a brief review of general fractional derivatives with memory effects and, in detail, deduce two important properties for these two kinds of general fractional derivative, which is helpful in constructing the unified framework for general fractional grey models in the following section.

Definition 1 (See [30]). *Given order $r \in (0, 1), t > t_0$, the general fractional derivative with memory effects in the Caputo sense is presented as*

$$D_{t_0, r}^{GC} f(t) = N(r) \int_{t_0}^t k(t - \tau, r) \frac{df(\tau)}{d\tau} d\tau, \quad (4)$$

where G and C represent the general definition and Caputo sense, respectively. $k(t - \tau, r)$ and $N(r)$ denote kernel function and normalization one, respectively.

Eq.(4) can be rewritten in the form of convolution as follows,

$$D_{t_0, r}^{GC} f(t) = N(r) k(\tau, r) * \frac{df(t)}{dt} \quad (5)$$

By taking different kernel functions and normalization ones, Eq.(5) can be transferred into diverse fractional derivatives, for example

$$\begin{aligned} D_{t_0, r}^{Caputo} f(t) &= \frac{1}{\Gamma(1-r)} \int_{t_0}^t (t-\tau)^{-r} \frac{df(\tau)}{d\tau} d\tau \\ &= \frac{1}{\Gamma(1-r)} t^{-r} * \frac{df(t)}{dt} \end{aligned} \quad (6)$$

Eq.(9) is the basic form of the Caputo fractional derivative.

Definition 2 (See [30]). Given $r \in (0, 1), t > t_0$, the general fractional derivative with memory effects in the Riemann–Liouville sense is represented as

$$D_{t_0, r}^{GRL} f(t) = \frac{d}{dt} N(r) \int_{t_0}^t k(t - \tau, r) f(\tau) d\tau, \quad (7)$$

where RL denotes the Riemann-Liouville sense, $k(t - \tau, r)$ and $N(r)$ are the same as in Definition 1.

Similar to Eq.(5), Eq.(7) can be expressed in the form of convolution as follows,

$$D_{t_0, r}^{GRL} f(t) = \frac{d}{dt} N(r) k(\tau, r) * f(t) \quad (8)$$

Meanwhile, Eq.(8) can be reduced to other fractional derivatives by taking different kernel functions and normalization ones, for example, the Riemann-Liouville fractional derivative is calculated as

$$\begin{aligned} D_{t_0, r}^{RL} f(t) &= \frac{df(t)}{dt} \frac{1}{\Gamma(1-r)} \int_{t_0}^t (t-\tau)^{-r} f(\tau) d\tau \\ &= \frac{df(t)}{dt} \frac{1}{\Gamma(1-r)} t^{-r*} f(t) \end{aligned} \quad (9)$$

Each fractional derivative has its own advantages and limitations, in addition, other kinds of the fractional derivative with diverse kernel functions and normalization ones are also shown in Ref.[30] and references therein.

3. Unified representation of fractional grey model

In this section, we present a unified framework for the general fractional grey models based on the above findings. In addition to analyze the characteristics of this framework, another focus is to deduce its time response function and structural parameters.

Assume $X^{(0)} = \{x^{(0)}(1), x^{(0)}(2), \dots, x^{(0)}(n)\}, n \geq 4$ to be a nonnegative sequence, and the α -order accumulated generating operation (α -FAGO) sequence is given as $X^{(\alpha)} = \{x^{(\alpha)}(1), x^{(\alpha)}(2), \dots, x^{(\alpha)}(n)\}$. then consider the general fractional grey model in the Caputo and Riemann-Liouville senses, namely UFGM, one has

$$N(r) \int_{t_0}^t k(t - \tau, r) \frac{dx^{(\alpha)}(\tau)}{d\tau} d\tau + ax^{(\alpha)}(t) = \psi(t) + c, \quad (10)$$

and

$$\frac{d}{dt} N(r) \int_{t_0}^t k(t - \tau, r) x^{(\alpha)}(\tau) d\tau + ax^{(\alpha)}(t) = \psi(t) + c \quad (11)$$

respectively, where $\psi(t)$ is the unknown function with respect to t and the discrete form of $x^{(\alpha)}(t)$ gives

$$x^{(\alpha)}(k) = \sum_{i=1}^k \binom{k-i+\alpha-1}{k-i} x^{(0)}(i), k = 1, 2, \dots, n, \quad (12)$$

where $\binom{k-i+\alpha-1}{k-i} = \frac{(\alpha+k-i-1)(\alpha+k-i-2)\dots(\alpha+1)\alpha}{(k-i)!}$. The fractional accumulation plays an important role in the construction of grey models. For more details on the accuracy analysis of fractional accumulation, see [10] for a review.

For simplicity, $\psi(t)$ is taken as $\psi(t) = bt + c$ and, Eqs.(10)-(11) become

$$N(r) \int_{t_0}^t k(t - \tau, r) \frac{dx^{(\alpha)}(\tau)}{d\tau} d\tau + ax^{(\alpha)}(t) = bt + c, \quad (13)$$

and

$$\frac{d}{dt}N(r) \int_{t_0}^t k(t-\tau, r)x^{(\alpha)}(\tau)d\tau + ax^{(\alpha)}(t) = bt + c. \quad (14)$$

Next, using the trapezoid formula gives the discrete-time equation of Eq.(13)

$$\nabla D_{t_0, r}^{GC}x^{(\alpha)}(k) + \frac{a}{2} \left\{ x^{(\alpha)}(k) + x^{(\alpha)}(k-1) \right\} = bk + c, k = 1, 2, 3, \dots, n \quad (15)$$

For the structural parameter estimation, set $\varphi = (a, b, c)^T$ and $f(x^{(\alpha)}(k), \varphi) = -\frac{a}{2}(x^{(\alpha)}(k) + x^{(\alpha)}(k-1)) + bk + c$, one has

$$\varphi = (a, b, c)^T = (\mathbf{A}^T \mathbf{A})^{-1} \mathbf{A}^T \mathbf{Y} \quad (16)$$

where

$$\mathbf{A} = \begin{bmatrix} \frac{\partial f(x^{(\alpha)}(2), \varphi)}{\partial a} & \frac{\partial f(x^{(\alpha)}(2), \varphi)}{\partial b} & \frac{\partial f(x^{(\alpha)}(2), \varphi)}{\partial c} \\ \frac{\partial f(x^{(\alpha)}(3), \varphi)}{\partial a} & \frac{\partial f(x^{(\alpha)}(3), \varphi)}{\partial b} & \frac{\partial f(x^{(\alpha)}(3), \varphi)}{\partial c} \\ \vdots & \vdots & \vdots \\ \frac{\partial f(x^{(\alpha)}(n), \varphi)}{\partial a} & \frac{\partial f(x^{(\alpha)}(n), \varphi)}{\partial b} & \frac{\partial f(x^{(\alpha)}(n), \varphi)}{\partial c} \end{bmatrix}, \mathbf{Y} = \begin{bmatrix} \nabla D_{t_0, r}^{GC}x^{(\alpha)}(2) \\ \nabla D_{t_0, r}^{GC}x^{(\alpha)}(3) \\ \vdots \\ \nabla D_{t_0, r}^{GC}x^{(\alpha)}(n) \end{bmatrix}, \quad (17)$$

and $\nabla D_{t_0, r}^{GC}x^{(\alpha)}(k)$ represents the discrete form of $D_{t_0, r}^{GC}x^{(\alpha)}(k)$. It is worth noting that the structural parameter estimation of Eq.(14) has been omitted because of their high similarity.

Theorem 1. Set $\mathcal{L}^{-1} \left\{ \frac{1}{[N(r)K(s, r)s + a]} \right\} = \Theta(r, t, a)$ and j indicates the discrete variable corresponding to t , the exact solution of Eq.(13) is expressed as

$$\hat{x}^{(\alpha)}(j) = \Theta(r, j, a) * jb + \Theta(r, j, a) * c + \hat{x}^{(\alpha)}(0)N(r)k(j, r) * \Theta(r, j, a), \quad (18)$$

where

$$\hat{x}^{(\alpha)}(0) = \frac{x^{(\alpha)}(1) - \Theta(r, 1, a) * b + \Theta(r, 1, a) * c}{N(r)k(1, r) * \Theta(r, 1, a)}, \quad (19)$$

$\mathcal{L}^{-1} \{.\}$ denotes the inverse Laplace transform. $\hat{x}^{(r)}(j)$ is the output value by the prediction model.

Proof. By applying the Laplace transform of general fractional derivative mentioned in [30], one has

$$N(r) \left\{ sX(s) - x^{(\alpha)}(0) \right\} K(s, r) + aX(s) = \frac{b}{s^2} + \frac{c}{s}, \quad (20)$$

Let $\frac{1}{[N(r)K(s, r)s + a]} = \Xi(r, s, a)$, Eq.(20) becomes

$$X(s) = \frac{b}{s^2} \Xi(r, s, a) + \frac{c}{s} \Xi(r, s, a) + x^{(\alpha)}(0)K(s, r)N(r)\Xi(r, s, a), \quad (21)$$

Subsequently, through the inverse Laplace transform, Eq.(21) yields

$$\begin{aligned} x^{(\alpha)}(t) &= \mathcal{L}^{-1} \{ \Xi(r, s, a) \} * tb + \mathcal{L}^{-1} \{ \Xi(r, s, a) \} * c \\ &+ x^{(\alpha)}(0)N(r)\mathcal{L}^{-1} \{ K(s, r) \} * \mathcal{L}^{-1} \{ \Xi(r, s, a) \} \end{aligned} \quad (22)$$

where $\mathcal{L} \{ \hat{x}^{(\alpha)}(t) \} = X(s)$. Then substituting Eq.(22) into Eq.(20), one can write

$$\hat{x}^{(\alpha)}(t) = \Theta(r, t, a) * tb + \Theta(r, t, a) * c + \hat{x}^{(\alpha)}(0)N(r)k(t, r) * \Theta(r, t, a). \quad (23)$$

Set $\hat{x}^{(\alpha)}(1) = x^{(\alpha)}(1)$ and $j = t$, this completes the proof. \square

Theorem 2. The exact solution of Eq.(14) is expressed as

$$\hat{x}^{(\alpha)}(t) = \Theta(r, t, a) * tb + \Theta(r, t, a) * c + x^{(\alpha)}(0)N(r)k(x, r) * \Theta(r, t, a) \quad (24)$$

where $\hat{x}^{(\alpha)}(0) = \frac{x^{(\alpha)}(1) - \Theta(r, 1, a) * b + \Theta(r, 1, a) * c}{N(r)k(x, r) * \Theta(r, 1, a)}$ and $\mathcal{L}^{-1} \left\{ \frac{1}{N(r)K(s, r)s + x^{(\alpha)}(0) + a} \right\} = \Theta(r, t, a)$.

Proof. By applying the link between the GC and GRL derivatives in [30]

$$D_{r, t_0}^{GC} f(t) = D_{r, t_0}^{GRL} x^{(\alpha)}(t) - N(r)x^{(\alpha)}(0)k(x, r) \quad (25)$$

Thus, Eq.(14) is rearranged as

$$D_{r, t_0}^{GC} x^{(\alpha)}(t) + N(r)x^{(\alpha)}(0)k(x, r) + ax^{(\alpha)}(t) = bt + c \quad (26)$$

By applying the laplace transform on both sides of Eq. (26), we obtain

$$N(r) \left\{ sX(s) - x^{(\alpha)}(0) \right\} K(s, r) + x^{(\alpha)}(0)X(s) + aX(s) = \frac{b}{s^2} + \frac{c}{s} \quad (27)$$

Set $\frac{1}{\{N(r)K(s, r)s + x^{(\alpha)}(0) + a\}} = \mathcal{W}(r, s, a)$, it follows that

$$X(s) = \mathcal{W}(r, s, a) \frac{b}{s^2} + \mathcal{W}(r, s, a) \frac{c}{s} + x^{(\alpha)}(0)N(r)K(s, r)\mathcal{W}(r, s, a) \quad (28)$$

and

$$\begin{aligned} \hat{x}^{(\alpha)}(t) &= \mathcal{L}^{-1} \{ \mathcal{W}(r, s, a) \} * tb + \mathcal{L}^{-1} \{ \mathcal{W}(r, s, a) \} * c \\ &+ x^{(\alpha)}(0)N(r)\mathcal{L}^{-1} \{ K(s, r) \} * \mathcal{L}^{-1} \{ \mathcal{W}(r, s, a) \} \end{aligned} \quad (29)$$

where $\mathcal{L}^{-1} \{ \mathcal{W}(r, s, a) \} = \Theta(r, t, a)$. Finally, set $\hat{x}^{(\alpha)}(1) = x^{(\alpha)}(1)$ and $s = t$, the exact solution (often called time response function) of Eq.(24) can be easily obtained. \square

Remark 1. Set $k(t - \tau, r) = e^{-\frac{r}{1-r}x}$ and $N(r) = 1$ [29], a novel fractional grey model is presented as

$${}_0^{\text{exp}}D_t^r x^{(\alpha)}(t) + ax^{(\alpha)}(t) = bt + c. \quad (30)$$

By applying the laplace transformation on Eq.(3), which yields that

$$\mathcal{L} \left\{ {}_0^{\text{exp}}D_t^r x^{(\alpha)} \right\} + \mathcal{L} \left\{ ax^{(\alpha)}(t) \right\} = \mathcal{L} \{ bt \} + \mathcal{L} \{ c \}$$

and

$$\frac{sX(s) - x^{(\alpha)}(0)}{s + r(1 - s)} + aX(s) = \frac{b}{s^2} + \frac{c}{s} \quad (31)$$

By further solving Eq.(31), one can write

$$X(s) = \frac{crs^2 + brs - crs - cs^2 - x^{(\alpha)}(0)s^2 - br - bs}{s^2(ars - ar - as - s)} \quad (32)$$

The continuous solution to Eq.(32) can be calculated by the inverse laplace transformation operation, which is as follows,

$$\hat{x}^{(\alpha)}(t) = \frac{b \left(\frac{art}{ar-a-1} - 1 \right)}{a^2r} + \frac{bt(ar - a - 1) + e^{\frac{art}{ar-a-1}}(-ax + c) + c(ar - a - 1)}{(ar - a - 1)a} \quad (33)$$

Set $\hat{x}^{(\alpha)}(1) = x^{(\alpha)}(1)$ and $t = k$, the discrete time response function of can be given as

$$\hat{x}^{(\alpha)}(k) = \left(x^{(\alpha)}(1) - \frac{b}{a} - \frac{c}{a} + \frac{b}{a^2 r} \right) e^{\frac{-ar(k-1)}{1-ar+a}} + \frac{b}{a} k + \frac{c}{a} - \frac{b}{a^2 r} \quad (34)$$

Remark 2. Inspired by the idea in [28], the discrete form of Eq.(3) is $x^{(\alpha-r)}(k) + \frac{a}{2} \{x^{(\alpha)}(k-1) + x^{(\alpha)}(k)\} = bk + c$. Subsequently we estimate the structural parameters by constructing a cost function expressed as

$$\chi^2 = \sum_{k=2}^n \left\{ x^{(\alpha-r)}(k) + az^{(\alpha)}(k) - bk - c \right\}^2 \quad (35)$$

And by minimizing χ^2 , one has a set of equations with respect to partial function expressed as

$$\begin{cases} \frac{\partial \chi^2}{\partial a} = \sum_{k=2}^n 2z^{(\alpha)}(k)x^{(\alpha-r)}(k) + 2a\{z^{(\alpha)}(k)\}^2 - 2z^{(\alpha)}(k)bk - 2z^{(\alpha)}(k)c = 0, \\ \frac{\partial \chi^2}{\partial b} = \sum_{k=2}^n -2kx^{(\alpha-r)}(k) - 2kaz^{(\alpha)}(k) + 2k^2b + 2kc = 0, \\ \frac{\partial \chi^2}{\partial c} = \sum_{k=2}^n -2x^{(\alpha-r)}(k) - 2az^{(\alpha)}(k) + 2bk + 2c = 0. \end{cases} \quad (36)$$

which yields that

$$\begin{cases} \sum_{k=2}^n a\{z^{(\alpha)}(k)\}^2 - \sum_{k=2}^n z^{(\alpha)}(k)bk - \sum_{k=2}^n z^{(\alpha)}(k)c = -\sum_{k=2}^n z^{(\alpha)}(k)x^{(\alpha-r)}(k), \\ -\sum_{k=2}^n kaz^{(\alpha)}(k) + \sum_{k=2}^n k^2b + \sum_{k=2}^n kc = \sum_{k=2}^n kx^{(\alpha-r)}(k), \\ -\sum_{k=2}^n az^{(\alpha)}(k) + \sum_{k=2}^n bk + \sum_{k=2}^n c = \sum_{k=2}^n x^{(\alpha-r)}(k). \end{cases} \quad (37)$$

and then, using the least squares, the structural parameter estimates give in matrix form expressed as

$$(a, b, c)^T = (\mathcal{O}^T \mathcal{O})^{-1} \mathcal{O}^T \mathbf{H} \quad (38)$$

where

$$\mathcal{O} = \begin{pmatrix} \sum_{k=2}^n \{z^{(\alpha)}(k)\}^2 & -\sum_{k=2}^n z^{(\alpha)}(k)k & -\sum_{k=2}^n z^{(\alpha)}(k) \\ -\sum_{k=2}^n kz^{(\alpha)}(k) & \sum_{k=2}^n k^2 & \sum_{k=2}^n k \\ -\sum_{k=2}^n z^{(\alpha)}(k) & \sum_{k=2}^n k & \sum_{k=2}^n 1 \end{pmatrix}$$

$$\mathbf{H} = \begin{pmatrix} -\sum_{k=2}^n z^{(\alpha)}(k)x^{(\alpha-r)}(k) \\ -\sum_{k=2}^n kx^{(\alpha-r)}(k) \\ -\sum_{k=2}^n x^{(\alpha-r)}(k) \end{pmatrix}$$

Substituting the estimates of the structural parameters and initial value $\hat{x}^{(\alpha)}(1) = x^{(0)}(1)$ into Eq.(34), the restored values of the original sequence can be given by then using the inverse fractional accumulated generating operation

$$\hat{x}^{(0)}(k) = \sum_{i=1}^k \binom{k-i+1-\alpha-1}{k-i} \hat{x}^{(\alpha)}(i) - \sum_{i=1}^{k-1} \binom{k-1-i+1-\alpha-1}{k-i-1} \hat{x}^{(\alpha)}(i) \quad (39)$$

We recall the above remarks, where Remark 1 shows that the unified model has the flexibility to present the continuous fractional grey models and integer-order grey models. For instance, if fractional accumulation order α is taken as “1”, Eq.(34) is simplified as the basic form of NHGM(1,1) [3], whose

time response function is presented as $\hat{x}^{(\alpha)}(k) = (x^{(\alpha)}(0) - \frac{b}{a} - \frac{c}{a} + \frac{b}{a^2}) e^{-a(k-1)} + \frac{b}{a}k + \frac{c}{a} - \frac{b}{a^2}$. Remark 2, in detail, introduces the calculation process of the least squares in the special example, which help readers better understand the relevant calculation mechanism. Remarks 1-2 also introduce the possibility of developing some other novel fractional models.

4. Simulation studies

For the purpose of numerically analyzing the prediction performance of the unified model (i.e., UFGM(1,1)), we carry out the experiments from the diverse two aspects: One is to compare the prediction results by UFGM(1,1) with those by other benchmarks including the GM(1,1) [1], DGM(1,1) [3], FGM(1,1) [10] and ANN [45] models; another is to explore the impact of initial value and fractional accumulation order on the prediction accuracy of UFGM(1,1).

4.1. Validity of the UFGM(1,1) model

Three error-value metrics are chosen to evaluate the accuracy of UFGM(1,1), which embrace the mean absolute percentage error (MAPE), mean square error (MSE) and mean absolute error (MAE), which are defined, respectively, as follows,

$$MAPE = \frac{1}{n} \sum_{k=1}^n \frac{|\hat{x}^{(0)}(k) - x^{(0)}(k)|}{x^{(0)}(k)} \times 100\% \quad (40)$$

$$MSE = \frac{1}{n} \sum_{k=1}^n \left(\hat{x}^{(0)}(k) - x^{(0)}(k) \right)^2 \quad (41)$$

$$MAE = \frac{1}{n} \sum_{k=1}^n \left| \hat{x}^{(0)}(k) - x^{(0)}(k) \right| \quad (42)$$

For the experimental design, we consider 20 data sets, collected from the National Bureau of Statistics of China (<http://www.stats.gov.cn/>), as the inputs to calibrate models, which describes the electricity consumption in 20 provinces of China from 2014 to 2019. In UFGM(1,1), the emerging coefficients (i.e., r , α) plays an important role in the modeling process and more importantly, has a directly impact on the prediction accuracy. Thus we utilize the four commonly-used intelligent techniques, namely the grey wolf optimizer (GWO) [46], whale optimization algorithm (WOA) [47], particle swarm optimization (PSO) [48] and ant lion optimization (ALO) [49], to determine the optimal emerging coefficients for UFGM(1,1). For intuition, the fitting results produced by UFGM(1,1) with the help of the different algorithms are plotted in Figure 1.

Figure 1 shows that there is no fixed algorithm that enables UFGM(1,1) to produce the highest accuracy in all data sets, the reason for this situation is that each algorithm has its own advantages and limitations, thus it is possible to obtain better solutions for different problems. In the following analysis, it is necessary to evaluate the fitness value of these algorithms in each experiment, and the optimal emerging coefficients are chosen for model calibration. By reference with the current study and other published papers related to benchmarks, their comparative results are shown in Table 2. As table shows, the MAPE and MAE values of UFGM(1,1) are all smaller than those of other competitors, although its MSE values are slightly higher than traditional fractional grey model in several experiments, inferring that the UFGM(1,1) model outperforms other benchmarks in terms of model's prediction performance.

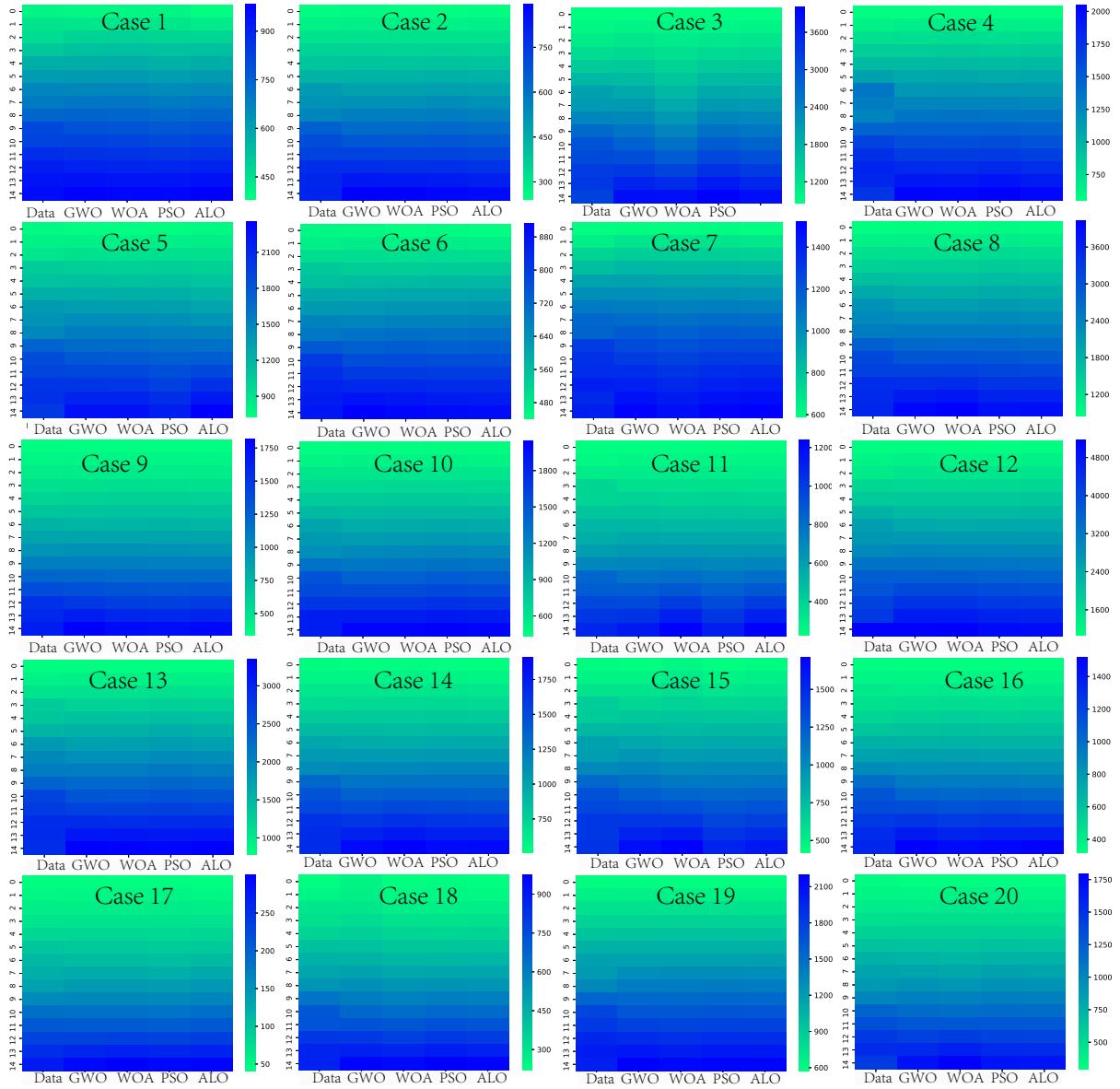


Figure 1: Prediction performance of the different algorithms-based UFGM(1,1) model

Table 2: Errors by the five competitive models in 20 data sets.

Case	Region	Metrics	GM(1,1)	DGM(1,1)	ANN	FGM(1,1)	UFGM(1,1)
1	Beijing	MAPE	4.4274	4.4237	3.362543	1.6294	1.4879
		MSE	1046	1047.3	826.1047	210.14	235.57
		MAE	27.941	27.86	24.12434	11.186	10.614
2	Tianjin	MAPE	4.4274	6.1891	3.132174	3.8301	2.404
		MSE	1046	1312.1	495.232	533.62	646.51
		MAE	27.941	28.989	18.21007	20.381	15.52
3	Hebei	MAPE	10.76	10.854	4.81092	7.9273	4.0727
		MSE	54708	54986	14763.99	29176	33992
		MAE	188.23	188.5	108.4177	149.38	104.99
4	Shanxi	MAPE	10.596	10.669	6.432003	6.8308	4.5779
		MSE	17969	18005	9898.418	8890.9	9452.1
		MAE	113.37	113.58	87.11586	81.838	65.915
5	Liaoning	MAPE	5.7687	4.88467	3.135815	4.0297	3.0828
		MSE	10219	8775.161	6730.438	4893.4	6243.1
		MAE	77.149	75.33215	66.32129	59.219	48.428
6	Heilongjiang	MAPE	2.4237	2.4298	2.524523	2.054	1.6633
		MSE	510.6	510.81	511.9586	291.74	260.93
		MAE	16.947	16.962	18.7526	14.031	12.103
7	Shanghai	MAPE	7.5002	7.5101	2.947381	2.9327	2.1168
		MSE	6967.2	6971.7	1679.166	1439.8	999.77
		MAE	72.783	72.7	33.71344	31.477	23.533
8	Zhejiang	MAPE	10.609	10.652	3.280667	5.1743	3.1869
		MSE	47904	48199	9964.663	13238	14965
		MAE	183.32	182.89	85.00789	100.01	84.197
9	Anhui	MAPE	5.6001	5.6303	5.0247	4.2216	2.125
		MSE	3372	3449	3805.964	2134.8	1828.6
		MAE	44.015	43.871	53.12803	35.507	24.597
10	Fujian	MAPE	6.5022	6.5479	4.896582	3.9373	2.0374
		MSE	5766.2	5839.6	5161.624	2369.6	2138.1
		MAE	56.337	56.409	57.57798	41.634	27.153
11	Jiangxi	MAPE	6.1053	6.1617	4.425646	3.7039	2.7821
		MSE	1254.7	1281.8	1303.201	574.3	641.04
		MAE	27.619	27.768	28.03915	19.493	16.943
12	Shandong	MAPE	7.1293	7.1613	5.36149	3.0638	2.9972
		MSE	31808	32177	36099.57	16175	15496
		MAE	148.94	148.89	160.1942	91.306	90.343
13	Henan	MAPE	9.5074	9.5784	4.283333	5.791	3.7368
		MSE	34638	34792	9638.134	15935	21391
		MAE	155.34	155.53	85.30263	104.06	86.514
14	Hubei	MAPE	5.9726	6.018	4.077524	4.4207	2.6483
		MSE	5783	5809.9	3683.539	3511.3	2765.1
		MAE	60.408	60.544	49.47484	47.658	34.901
15	Hunan	MAPE	7.1714	7.2392	5.419488	4.7514	3.7075
		MSE	5898.6	5922.9	4106.629	3018.3	3426.1
		MAE	62.315	62.555	55.92601	45.21	41.214
16	Guangxi	MAPE	7.3815	7.4647	4.084182	5.8011	3.3829
		MSE	4063.5	4111	1579.356	2460.7	2418.8
		MAE	50.793	50.964	35.79186	41.435	30.92
17	Hainan	MAPE	6.6034	6.6737	4.084182	3.5861	2.3553
		MSE	65.205	69.117	1579.356	25.571	26.381
		MAE	6.4182	6.4535	35.79186	4.2047	3.6773
18	Chongqing	MAPE	4.9022	4.9783	3.78875	4.5603	2.9425
		MSE	1036.4	1048.1	726.5574	796.52	775.06
		MAE	22.673	22.88	22.4828	21.756	17.092
19	Sichuan	MAPE	5.9849	6.0382	4.378797	4.1841	2.6998
		MSE	8572.9	8615	6206.165	4955.6	3959.6
		MAE	71.844	72.127	65.22631	58.053	42.153
20	Yunnan	MAPE	8.4035	8.5588	5.935477	7.3737	3.5109
		MSE	7395.2	7500.6	6465.405	5041.9	4563.6
		MAE	59.009	59.653	58.08669	58.986	36.112

4.2. Effects of fractional accumulation order and initial value on modelling

In order to explore the effects of fractional accumulation order and initial value on modelling, the initial value is sampled at every interval of 200000 in the range of $[1, 800000]$, and then r , α , a , b , c are all controlled within $[0, 1]$, of which the step is 0.2. Consider the data on total population at the end of the year (10^4 persons) from the National Bureau of Statistics of China (<http://www.stats.gov.cn/>). The pseudo-code for the relevant calculations are shown in Algorithm 1.

Algorithm 1: Effects of the fractional accumulation order and initial value on the prediction performance.

Input: Raw data $X^{(0)} = \{x^{(0)}(1), x^{(0)}(2), \dots, x^{(0)}(n)\}$

Output: Simulation value $\hat{x}^{(0)}(k)$

```

1 Initialize MAPEmin = + inf for Initial value = 1 to 800000 Step = 200000 do
2   for  $\alpha = 0.1$  to 1 Step = 0.2 do
3     for  $r = 0.1$  to 1 Step = 0.2 do
4       for  $a = 0.1$  to 1 Step = 0.2 do
5         for  $b = 0.1$  to 1 Step = 0.2 do
6           for  $c = 0.1$  to 1 Step = 0.2 do
7             Calculating  $X^{(\alpha)} = (x^{(\alpha)}(1), x^{(\alpha)}(2), \dots, x^{(\alpha)}(n))$  using the Eq.(12);
8             Calculating  $\hat{x}^{(\alpha)}(k)$  using the Eq.(34);
9             Calculate the fitting results  $\hat{x}^{(0)}(k)$  using Eq.(39);
10            Calculate the error of this model using the Eq.(40);
11 return  $\hat{x}^{(0)}(k)$ ;

```

Figure 2 shows that with the increase of the initial condition value, the MAPE values get larger when the other conditions are fixed, for example, $r = 0.1$ and $\alpha = 0.1$, inferring the predicted values by the UFGM(1,1) model deviate from the actual ones. In return, in the small initial value scenario, the smaller the fractional accumulation order, the lower the fitting error (i.e., MAPE); with the increase of the initial value, the fractional accumulation order should properly increase so as to better mine the characteristics hidden in the original sequence, for example, $r = \alpha = 0.3$ enables this model to provide the more accurate forecasts rather than that of $r = \alpha = 0.1$ in the large initial value scenario (i.e., *initial value* = 800000).

5. Application

Foresight of water supply capacity is of great significance for the sustainable development of society, is conducive to the rational distribution of water resources, and plays an important role in the development of the national economy. In this section, we further apply the UFGM(1,1) model to deal with the data on water supply production capacity (ten thousand cubic meters/day) in Henan and Chongqing, respectively. The prediction performance of the UFGM(1,1) model will be compared with the above benchmarks in terms of MAPE (elaborated on in Section 4.1). The total amount of water supply production capacity is collected from the National Bureau of Statistics of China (<http://www.stats.gov.cn/>), as shown in Tables 3-4.

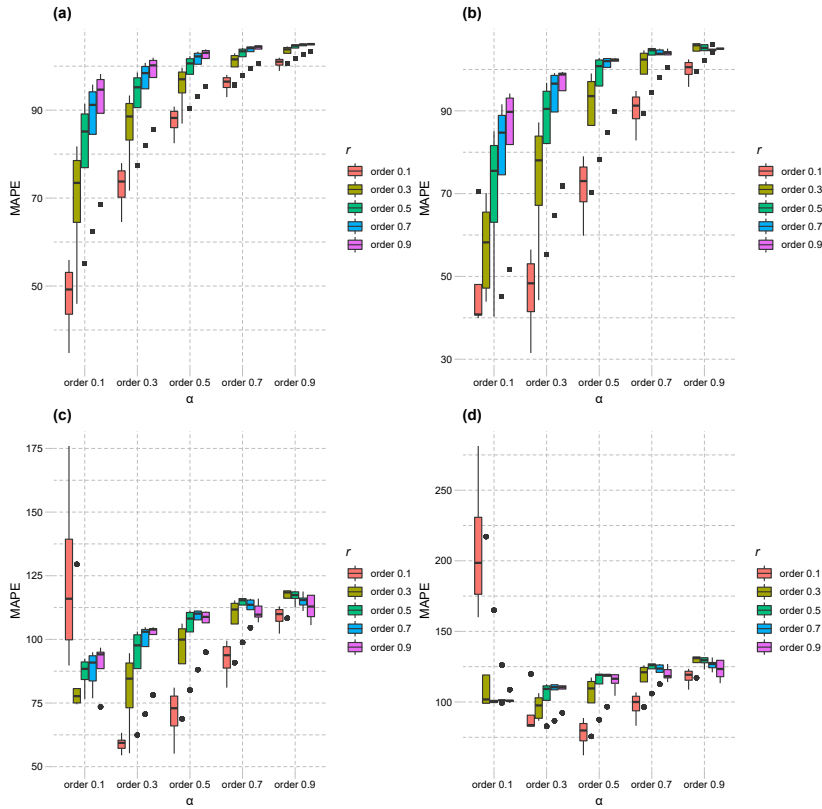


Figure 2: Effects of the fractional order accumulation order r, α on the UFGM(1,1) model in the four initial value scenarios: (a) *initial value = 1*; (b) *initial value = 200001*; (c) *initial value = 400001*; (d) *initial value = 600001*;

Case 1. (Forecasting Henan’s water supply production capacity) We consider the total amount of water supply production capacity from 2004 to 2019, in which the data from 2004 to 2015 are used for model calibration, and the left four samples are used to examine the accuracy. For the purpose of obtaining the optimal emerging coefficients for the UFGM(1,1) model, the four algorithms are carried out in this experiments, thus the track of searching process by the different algorithms is graphed in Figure 3. Subsequently, the minimum MAPE corresponding to the algorithm is applied to determine the emerging coefficients.

From Table 3, it is found that the MAPE value of UFGM(1,1) in the in-sample period is 0.91541%, while that of competitive models, namely GM(1,1), DGM(1,1), ANN and FGM(1,1), are 1.9183%, 1.9171%, 2.319511%, and 0.65119%, respectively, indicating the FGM(1,1) and UFGM(1,1) models have the higher accuracy in this stage because their MAPE values are closer to zeros. As for the out-of-sample period, the MAPE values of the current model and benchmarks are 2.8704%, 7.8142%, 7.8292%, 4.386027% and 14.2690%, respectively. It is obvious that the MAPE value of the UFGM(1,1) model is far less than others, this means the UFGM(1,1) model achieves the precise prediction in this experiment. The same finding can be also obtained from Figure 4.

Case 2. (Forecasting Chongqing’s water supply production capacity.) Similar to case one, the raw data is divided into two groups, one, training set, from 2004 to 2015 are used for calibrating structural parameters; another, testing set, from 2016 to 2019 are used to evaluate the prediction performance. First and foremost, according to the performance of the four algorithms on the determination of emerging

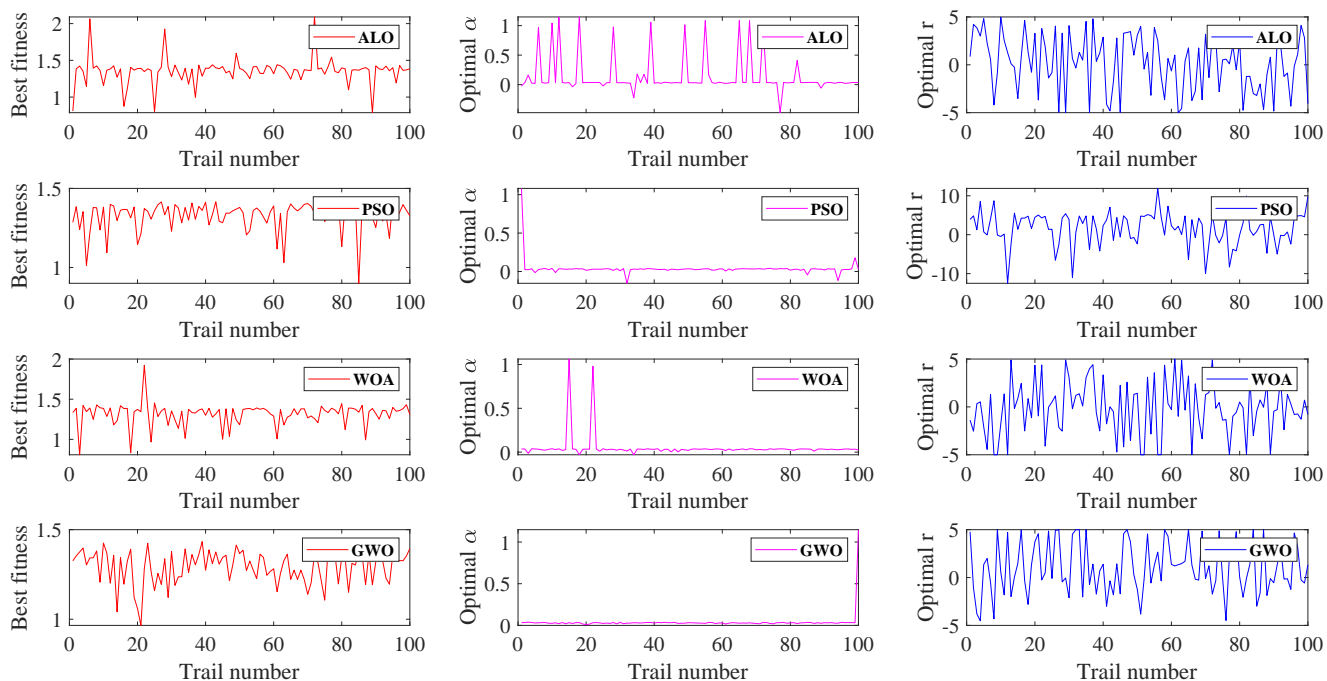


Figure 3: r , α and the fitness value of the UFGM(1,1) model in each trial by using the four algorithms in Case 1.

Table 3: Simulated and predicted values by the five competitive models in Case 1.

Raw data	GM(1,1)	Error(%)	DGM(1,1)	Error(%)	ANN	Error(%)	FGM(1,1)	Error(%)	UFGM(1,1)	Error(%)
In-sample										
1038.31	1038.31	0.000	1003.8	3.32367	1038.31	0.0000	1038.31	0.000	1038.31	0.000
1026.51	1003.7	2.222092	1003.8	2.212351	1026.51	0.0000	1026.8	0.028251	1022.9	0.351677
1023.7	1011	1.240598	1011.1	1.230829	1023.7	0.0000	1021.8	0.185601	1014.9	0.859627
1039.85	1018.4	2.062798	1018.5	2.053181	1039.85	0.0000	1019.3	1.976247	1011.5	2.726355
1013.91	1025.9	1.182551	1026	1.192414	1047.962	3.358434	1018.7	0.472429	1011.9	0.198242
1007.79	1033.4	2.541204	1033.5	2.551127	1042.344	3.42871	1019.8	1.191717	1015.9	0.804731
1010.34	1041	3.034622	1041	3.034622	1039.884	2.924204	1023.1	1.262941	1023.3	1.282737
1037.56	1048.6	1.064035	1048.6	1.064035	1031.243	0.608813	1029.3	0.796099	1033.9	0.352751
1042.31	1056.3	1.342211	1056.3	1.342211	1034.192	0.778837	1039.8	0.240811	1047.6	0.507527
1047.26	1064.1	1.608006	1064	1.598457	1042.544	0.450299	1056.4	0.872754	1064.5	1.646201
1083.62	1071.9	1.08156	1071.8	1.090788	1055.567	2.588786	1082.1	0.140271	1084.3	0.062753
1121.39	1079.7	3.717707	1079.6	3.726625	1071.847	4.417999	1121.4	0.000892	1107.1	1.274311
MAPE		1.9183		1.9171		2.319511		0.65119		0.91541
Out-of-sample										
1180.32	1087.6	7.855497	1087.5	7.863969	1093.27	7.375093	1181.1	0.066084	1132.8	4.026027
1150.37	1095.6	4.761077	1095.5	4.76977	1132.02	1.595139	1271.4	10.52096	1161.3	0.950129
1166.64	1103.7	5.39498	1103.5	5.412124	1157.322	0.798721	1407.6	20.65419	1192.6	2.225194
1281.52	1111.7	13.25145	1111.5	13.26706	1181.88	7.77515	1612.6	25.83495	1226.7	4.277733
MAPE		7.8142		7.8292		4.386027		14.26904		2.8704

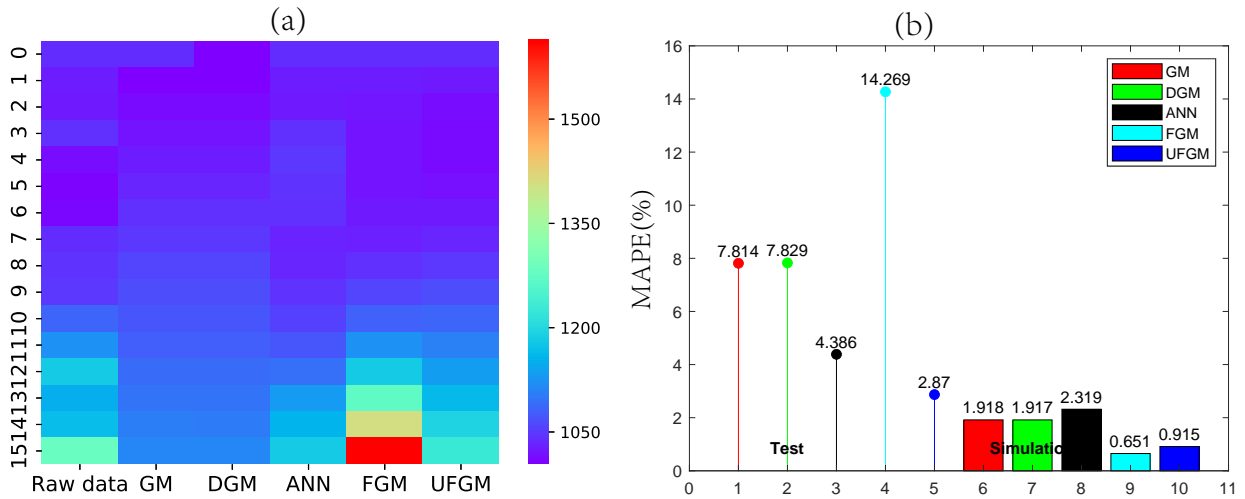


Figure 4: Prediction performance of the five competitors in Case 1: (a) Simulated and predicted values by the competitors; (b) Errors by the competitors.

coefficients shown in Figure 5, it is found that the fitness value by PSO is smallest, this means the emerging coefficients of UFGM(1,1) model will be determined by this algorithm. Subsequently, the prediction results by these competitive models are obtained by reference with the current study and references therein, as shown in Table 4. Meanwhile, these values in Table 4 are vividly displayed in Figure 6.

Table 4: Simulated and predicted results by the five competitive models in Case 2

Raw data	GM(1,1)	Error(%)	DGM(1,1)	Error(%)	ANN	Error(%)	FGM(1,1)	Error(%)	UFGM	Error(%)
In-sample										
373.65	373.65	0.000	373.65	0.000	373.65	0.000	373.65	0.000	373.65	0.000
405.61	381.59	5.921945	381.79	5.872636	405.61	0.000	380.87	6.099455	403.23	0.586771
391.7	392.78	0.275721	392.96	0.321675	391.7	0.000	389.02	0.684197	396.63	1.258616
419.2	404.31	3.552004	404.46	3.516221	419.2	0.000	398.22	5.004771	393.74	6.073473
418.16	416.17	0.475894	416.29	0.447197	431.3829	3.162163	408.6	2.286206	398.61	4.675244
420.35	428.38	1.910313	428.47	1.931724	435.0692	3.501649	420.32	0.007137	409.54	2.571666
412.3	440.94	6.946398	441	6.960951	441.3492	7.045642	433.55	5.154014	424.63	2.990541
429.27	453.88	5.732989	453.9	5.737648	437.3996	1.89382	448.47	4.472709	442.55	3.093624
447.83	467.2	4.325302	467.18	4.320836	446.0885	0.388882	465.31	3.903267	462.45	3.264632
491.22	480.9	2.100892	480.85	2.11107	459.6022	6.436593	484.32	1.404666	483.83	1.504418
506.89	495.01	2.343704	494.92	2.361459	493.1399	2.712648	505.78	0.218982	506.36	0.104559
529.92	509.53	3.847751	509.4	3.872283	516.7286	2.489319	529.99	0.01321	529.85	0.01321
MAPE		3.4031		3.4052		3.45384		2.6586		2.3759
Out-of-sample										
566.12	524.48	7.355331	524.3	7.387126	543.2325	4.042864	557.32	1.554441	554.15	2.114393
599.87	539.87	10.00217	539.64	10.04051	574.3076	4.26133	588.16	1.95209	579.16	3.452415
616.99	555.7	9.93371	555.43	9.977471	607.9011	1.473103	622.96	0.967601	604.82	1.972479
627.76	572.01	8.880782	571.68	8.93335	633.7528	0.954632	662.24	5.492545	631.08	0.528865
MAPE		9.043		9.0848		2.682982		2.4922		2.0169

Firstly, we observe from Table 4 and Figure 6 that for the in-sample period all of the competitors have a relatively satisfactory performance because their outputs of simulating and predicting Chongqing's water supply production capacity are close to actual ones. However, in the out-of-sample period, the predicted results by the GM(1,1) and DGM(1,1) models deviate from the actual ones although it fall within the acceptable range. Among these models, the UFGM(1,1) model have a higher accuracy because the

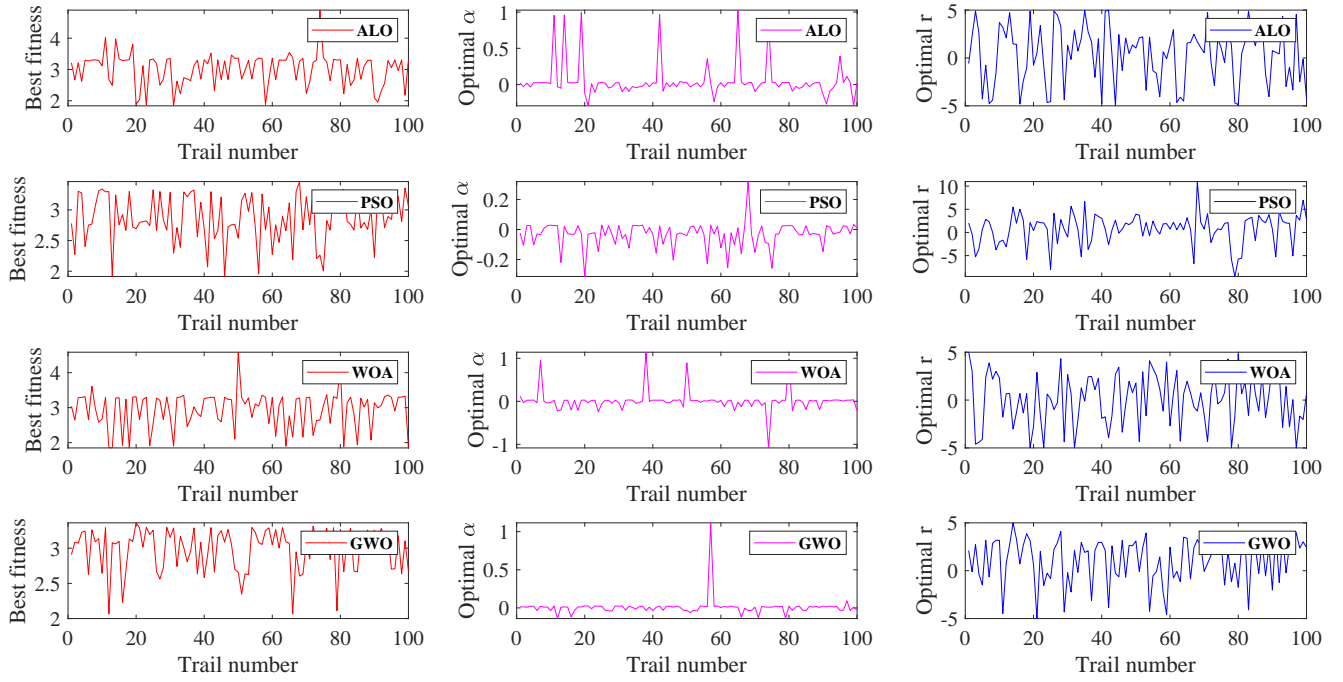


Figure 5: r , α and the fitness value of the UFGM(1,1) model in each trial by using the four algorithms in Case 2.

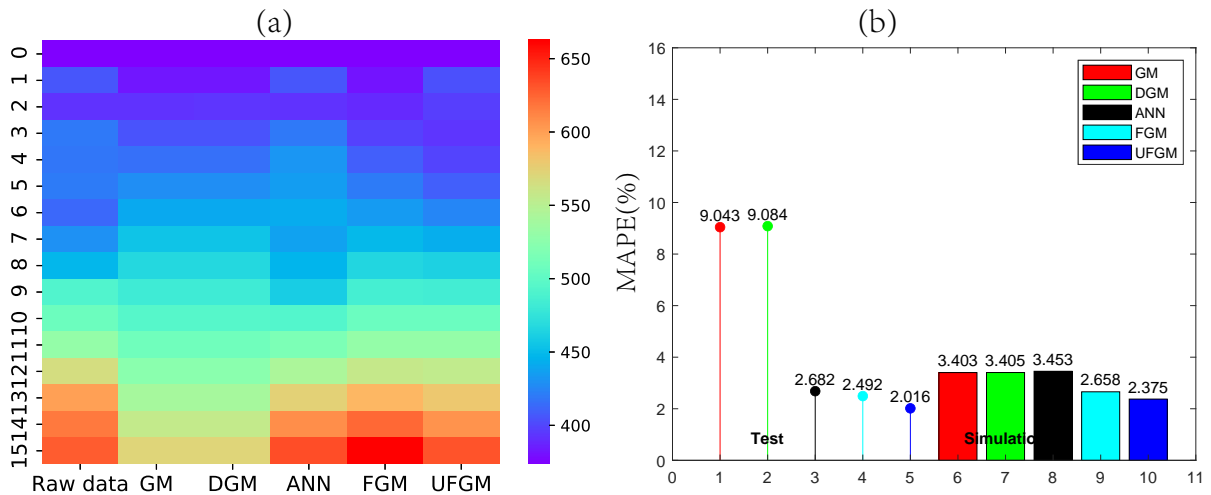


Figure 6: Prediction performance of the five competitors in Case 2: (a) Simulated and predicted values by the competitors; (b) Errors by the competitors.

corresponding prediction values are closer to the actual amount of Chongqing's water supply production capacity.

Next, the error-value indicator, i.e. MAPE, is applied to further analyze the prediction performance. In the simulation stage, the MAPE values of the UFGM(1,1) and other competitive models are 2.3759%, 3.4031%, 3.4052%, 3.45384% and 2.6586%, respectively; those of competitors are 2.01691%, 9.0431%, 9.08481%, 2.6829821% and 2.49221%, respectively, for the prediction stage. It is concluded that all of models are suitable for forecasting Chongqing's water supply production capacity in accordance with Lewis standard [50]. To be specific, the GM(1,1) and DGM(1,1) models have a relatively poor prediction accuracy due to their higher MAPEs, the UFGM(1,1) has a superiority over others because its MAPEs are smaller either in the in-sample or out-of-sample period. It is worth mentioned that the FGM(1,1) model has a second best performance due to its second smallest MAPE. In consequence, the UFGM(1,1) will be treated as an optimal tool for forecasting Chongqing's water supply production capacity in this experiment, and the FGM(1,1) model should be considered as a sub-optimal technique in dealing with Chongqing's water supply production capacity.

6. Conclusion and summary

In this study, an unified framework for fractional grey models is presented by combining general fractional derivative with memory effects and grey modeling theory. This unified framework (denoted as UFGM(1,1) for short) not just covers commonly-used fractional grey models already in place, but also can derived other new ones. The main conclusions are summarized as follows.

- Based on the GR and GRL fractional derivatives, the framework for published fractional grey models is developed. By taking different kernel functions and normalization ones, some other new fractional grey models can be deduced, a new fractional grey model, for example, with $k(x, r) = e^{-\frac{r}{1-r}x}$ and $N(r) = 1$, is expressed as ${}_0^{\text{exp}}D_t^\alpha x^{(\alpha)}(t) + ax^{(\alpha)}(t) = bt + c$.
- The commonly-used intelligent algorithms, namely GWO, PSO, WOA and ALO, are employed to search for the optimal emerging coefficients, i.e., r , and α , for the UFGM(1,1) model in the current study.
- Two published cases are utilized to verify the superiority of the UFGM(1,1) model and explore the effects of fractional accumulation order and initial value on the prediction performance.
- The UFGM(1,1) model is also applied to dealing with Henan's and Chongqing's water supply production capacity so as to explain the validity of the proposed method. Numerical results show that the UFGM(1,1) model outperforms a range of benchmarks.

In addition, the unified framework is not without limitations, for example, this framework is focusing on continuous-fractional grey models, potentially neglecting the discrete-fractional grey model (e.g. conformable fractional grey model [24]), this is a primary research direction of our following study. As stated in [51], the data-preprocessing techniques (e.g., data grouping [52], rolling mechanism [53], etc.) should be also worth exploring in the coming work.

Acknowledgements

This work was supported by the Postgraduate Research & Practice Innovation Program of Jiangsu Province (KYCX20_1144) and the Fundamental Research Funds for the Central Universities of China (Grant no. 2019YBZZ062).

References

References

- [1] J. L. Deng, Control problems of grey systems, *Systems & Control Letters* 1 (1982) 288-294.
- [2] N. Xie, R. Wang, A historic review of grey forecasting models., *Journal of grey System* 29 (2017).
- [3] N.-m. Xie, S.-f. Liu, Discrete grey forecasting model and its optimization, *Applied mathematical modelling* 33 (2009) 1173-1186.
- [4] M. Xia, W. Wong, A seasonal discrete grey forecasting model for fashion retailing, *Knowledge-Based Systems* 57 (2014) 119-126.
- [5] S. Ding, R. Li, Z. Tao, A novel adaptive discrete grey model with time-varying parameters for longterm photovoltaic power generation forecasting, *Energy Conversion and Management* 227 (2021) 113644.
- [6] L. Liu, L. Wu, Forecasting the renewable energy consumption of the european countries by an adjacent non-homogeneous grey model, *Applied Mathematical Modelling* 89 (2021) 1932-1948.
- [7] L. Ye, N. Xie, A. Hu, A novel time-delay multivariate grey model for impact analysis of co2 emissions from chinas transportation sectors, *Applied Mathematical Modelling* 91 (2021) 493-507.
- [8] X. Xiao, H. Duan, A new grey model for traffic flow mechanics, *Engineering Applications of Artificial Intelligence* 88 (2020) 103350.
- [9] S. A. Javed, B. Zhu, S. Liu, Forecast of biofuel production and consumption in top co2 emitting countries using a novel grey model, *Journal of Cleaner Production* 276 (2020) 123997.
- [10] L. Wu, S. Liu, L. Yao, S. Yan, D. Liu, Grey system model with the fractional order accumulation, *Communications in Nonlinear Science and Numerical Simulation* 18 (2013) 1775-1785.
- [11] Y. Yang, D. Xue, Continuous fractional-order grey model and electricity prediction research based on the observation error feedback, *Energy* 115 (2016) 722-733.
- [12] W. Zhou, X. Wu, S. Ding, J. Pan, Application of a novel discrete grey model for forecasting natural gas consumption: A case study of jiangsu province in china, *Energy* 200 (2020) 117443.
- [13] W. Wu, X. Ma, Y. Zhang, W. Li, Y. Wang, A novel conformable fractional non-homogeneous grey model for forecasting carbon dioxide emissions of brics countries, *Science of the Total Environment* 707 (2020) 135447.
- [14] W. Zhou, S. Ding, A novel discrete grey seasonal model and its applications, *Communications in Nonlinear Science and Numerical Simulation* 93 (2021) 105493.
- [15] Z.-X. Wang, Y.-Q. Jv, A novel grey prediction model based on quantile regression, *Communications in Nonlinear Science and Numerical Simulation* 95 (2021) 105617.

- [16] Q. Xiao, M. Shan, M. Gao, X. Xiao, M. Goh, Parameter optimization for nonlinear grey bernoulli model on biomass energy consumption prediction, *Applied Soft Computing* 95 (2020) 106538.
- [17] N. Li, J. Wang, L. Wu, Y. Bentley, Predicting monthly natural gas production in china using a novel grey seasonal model with particle swarm optimization, *Energy* 215 (2021) 119118.
- [18] B. Zeng, M. Tong, X. Ma, A new-structure grey verhulst model: development and performance comparison, *Applied Mathematical Modelling* 81 (2020) 522-537.
- [19] B. Wei, N. Xie, Parameter estimation for grey system models: A nonlinear least squares perspective, *Communications in Nonlinear Science and Numerical Simulation* 95 (2021) 105653.
- [20] L. Zeng, A novel discrete grey riccati model and its application, *Grey Systems: Theory and Application* (2020).
- [21] Q. Xiao, M. Gao, X. Xiao, M. Goh, A novel grey riccatiCbernoulli model and its application for the clean energy consumption prediction, *Engineering Applications of Artificial Intelligence* 95 (2020) 103863.
- [22] L.-F. Wu, S.-F. Liu, W. Cui, D.-L. Liu, T.-X. Yao, Non-homogenous discrete grey model with fractional-order accumulation, *Neural Computing and Applications* 25 (2014) 1215-1221.
- [23] W. Q. Wu, X. Ma, B. Zeng, Y. Wang, W. Cai, Forecasting short-term renewable energy consumption of China using a novel fractional nonlinear grey Bernoulli model, *Renewable Energy* 140 (2019) 70- 87.
- [24] X. Ma, W. Q. Wu, B. Zeng, Y. Wang, X. X. Wu, The conformable fractional grey system model, *ISA Transactions* (2019).
- [25] Y. Chen, W. Lifeng, L. Lianyi, Z. Kai, Fractional hausdorff grey model and its properties, *Chaos, Solitons & Fractals* 138 (2020) 109915.
- [26] L. Liu, Y. Chen, L. Wu, The damping accumulated grey model and its application, *Communications in Nonlinear Science and Numerical Simulation* 95 (2021) 105665.
- [27] L. Wu, S. Liu, L. Yao, Grey model with caputo fractional order derivative, *System Engineering Theory & Practice* 35 (2015) 1311C1316.
- [28] S. Mao, M. Gao, X. Xiao, M. Zhu, A novel fractional grey system model and its application, *Applied Mathematical Modelling* 40 (2016) 5063-5076.
- [29] S. Mao, Y. Kang, Y. Zhang, X. Xiao, H. Zhu, Fractional grey model based on non-singular exponential kernel and its application in the prediction of electronic waste precious metal content, *ISA transactions* 107 (2020) 12-26.
- [30] D. Zhao, M. Luo, Representations of acting processes and memory effects: General fractional derivative and its application to theory of heat conduction with finite wave speeds, *Applied Mathematics and Computation* 346 (2019) 531-544.
- [31] Y. Yang, D. Xue, An actual load forecasting methodology by interval grey modeling based on the fractional calculus, *ISA transactions* 82 (2018) 200-209.

- [32] L. Wu, X. Gao, Y. Xiao, Y. Yang, X. Chen, Using a novel multi-variable grey model to forecast the electricity consumption of shandong province in china, *Energy* 157 (2018) 327-335.
- [33] W. Q. Wu, X. Ma, B. Zeng, Y. Wang, W. Cai, Application of the novel fractional grey model FAGMO(1,1,k) to predict China's nuclear energy consumption, *Energy* 165 (2018) 223-234.
- [34] X. Ma, M. Xie, W. Wu, B. Zeng, Y. Wang, X. Wu, The novel fractional discrete multivariate grey system model and its applications, *Applied Mathematical Modelling* 70 (2019) 402-424.
- [35] L. Chen, Z. Liu, N. Ma, Optimize production allocation for the oil-gas field basing on a novel grey model, *Journal of Natural Gas Geoscience* 4 (2019) 121-128.
- [36] L. Wang, Y. Xie, X. Wang, J. Xu, H. Zhang, J. Yu, Q. Sun, Z. Zhao, Meteorological sequence prediction based on multivariate space-time auto regression model and fractional calculus grey model, *Chaos, Solitons & Fractals* 128 (2019) 203-209.
- [37] X. Ma, M. Xie, W. Q. Wu, X. X. Wu, B. Zeng, A novel fractional time delayed grey model with Grey Wolf Optimizer and its applications in forecasting the natural gas and coal consumption in Chongqing China, *Energy* 178 (2019) 487-507.
- [38] X. Zhu, Y. Dang, S. Ding, Using a self-adaptive grey fractional weighted model to forecast jiangsu's electricity consumption in china, *Energy* 190 (2020) 116417.
- [39] W. Xie, C. Liu, W.-Z. Wu, W. Li, C. Liu, Continuous grey model with conformable fractional derivative, *Chaos, Solitons & Fractals* 139 (2020) 110285.
- [40] K. Yuxiao, M. Shuhua, Z. Yonghong, Z. Huimin, Fractional derivative multivariable grey model for nonstationary sequence and its application, *Journal of Systems Engineering and Electronics* 31 (2020) 1009-1018.
- [41] M. Gao, H. Yang, Q. Xiao, M. Goh, A novel fractional grey riccati model for carbon emission prediction, *Journal of Cleaner Production* 282 (2021) 124471.
- [42] C. Liu, T. Lao, W.-Z. Wu, W. Xie, Application of optimized fractional grey model-based variable background value to predict electricity consumption, *Fractals* (2020).
- [43] Y. Zhang, S. Mao, Y. Kang, J. Wen, Fractal derivative fractional grey riccati model and its application, *Chaos, Solitons & Fractals* 145 (2021) 110778.
- [44] N. M. Xie, S. F. Liu, Y. J. Yang, C. Q. Yuan, On novel grey forecasting model based on nonhomogeneous index sequence, *Applied Mathematical Modelling* 37 (2013) 5059-6069.
- [45] S. S. Nain, P. Sihag, S. Luthra, Performance evaluation of fuzzy-logic and bp-ann methods for wedm of aeronautics super alloy, *MethodsX* 5 (2018) 890-908.
- [46] S. Mirjalili, S. M. Mirjalili, A. Lewis, Grey wolf optimizer, *Advances in engineering software* 69 (2014) 46-61.
- [47] S. Mirjalili, A. Lewis, The whale optimization algorithm, *Advances in engineering software* 95 (2016) 51-67.

- [48] F. Marini, B. Walczak, Particle swarm optimization (pso). a tutorial, *Chemometrics and Intelligent Laboratory Systems* 149 (2015) 153-165.
- [49] S. Mirjalili, The ant lion optimizer, *Advances in engineering software* 83 (2015) 80C98.
- [50] C. D. Lewis, *Industrial and business forecasting methods: A practical guide to exponential smoothing and curve fitting*, Butterworth-Heinemann, 1982.
- [51] B. Wei, N. Xie, On unified framework for discrete-time grey models: Extensions and applications, *ISA transactions* 107 (2020) 1-11.
- [52] Z.-X. Wang, Q. Li, L.-L. Pei, Grey forecasting method of quarterly hydropower production in china based on a data grouping approach, *Applied Mathematical Modelling* 51 (2017) 302-316.
- [53] X. Xiao, J. Yang, S. Mao, J. Wen, An improved seasonal rolling grey forecasting model using a cycle truncation accumulated generating operation for traffic flow, *Applied Mathematical Modelling* 51 (2017) 386-404.